Grueneberg Ganglion Cells Mediate Alarm Pheromone Detection in Mice

Julien Brechbühl, Magali Klaey, Marie-Christine Broillet*

Alarm pheromones (APs) are widely used throughout the plant and animal kingdoms. Species such as fish, insects, and mammals signal danger to conspecifics by releasing volatile alarm molecules. Thus far, neither the chemicals, their bodily source, nor the sensory system involved in their detection have been isolated or identified in mammals. We found that APs are recognized by the Grueneberg ganglion (GG), a recently discovered olfactory subsystem. We showed with electron microscopy that GG neurons bear primary cilia, with cell bodies ensheathed by glial cells. APs evoked calcium responses in GG neurons in vitro and induced freezing behavior in vivo, which completely disappeared when the GG degenerated after axotomy. We conclude that mice detect APs through the activation of olfactory GG neurons.

In a threatening situation, plants and animals warn conspecifics by secreting alarm pheromones (APs) (1–4). These substances signal injury, distress, or the presence of predators. In animals, the response of conspecifics to these signals is usually to freeze, attack, or disperse (5–7). Mammalian APs have not been identified yet; they may be low-molecular-weight volatile substances (8, 9), and it remains unknown whether their detection by conspecifics is mediated by a specialized olfactory subsystem.

In mammals, the most recently discovered olfactory subsystem (10–14), the so-called Grueneberg ganglion (GG) (15), is present at the tip of the nose, close to the opening of the naris, and is easy to observe in one particular gene-targeted mouse strain called OMP-GFP (olfactory marker protein–green fluorescent protein) (Fig. 1A). In these mice, a GFP-positive, arrow-shaped neuronal structure 750 to 1000 μm in length lines both sides of the nasal septum and comprises 300 to 500 cells (Fig. 1B). Each cell sends out a single axon, and axons fasciculate immediately (Fig. 1C) as they project caudally along the dorsal roof of the nasal cavity to the necklace complex in the olfactory bulb (10–12). The GG starts developing around embryonic day 16 and appears to be complete at birth (10–14).

Olfactory neurons sense the external chemical environment through the presence, at the end of their single dendrite, of cilia or microvilli in direct contact with the airspace of the nasal cavity. In contrast, under light or confocal microscopy, the mouse GG looks like a densely packed population of round cell bodies lacking these typical olfactory neuronal features or supporting glial cells (Fig. 1D) (11–14). GG cells express, in addition to OMP, molecular olfactory components. Indeed, extensive reverse transcription polymerase chain reaction and in situ hybridization analyses identified one vomeronasal organ (VNO) receptor, a distinct subtype of the V2R class, V2R83; and heterotrimeric GTP-binding proteins (G proteins) $G_{\alpha o}$ and $G_{\alpha i2}$ (16, 17). This suggests that the GG is in fact an olfactory subsystem with specific chemosensory functions.

To resolve the apparent contradiction between the lack of cilia or dendrites and a possible olfactory function of GG cells, we looked at the structure and cellular organization of the mouse GG by performing scanning electron microscopy (SEM) on coronal slices (Fig. 1, E to G). We found clusters of round GG cells in a fibroblast meshwork between the nasal septum and a keratinized epithelium (KE) (Fig. 1, E and F) (13). With this technical approach, four to eight ciliary processes were observed per GG cell (Fig. 1G). They were further characterized by transmission electron microscopy (TEM) (figs. S1 to S3) to be nonmotile primary cilia according to their microtubular characteristics (fig. S1, B and C) (18, 19). Thirty to forty primary cilia were present per GG cell, profoundly invaginated into the cytoplasm (5 μm) (fig. S1B) and grouped into three to four packs of 8 to 12 per cell (figs. S1C and S3). Analyzing serial ultrathin sections, we estimated both their length (15 μm) and their diameter (0.2 μm). Primary cilia were observed in the extracellular matrix (fig. S1, E to G) but not within the leaky KE, and they did not cross the keratin layers to
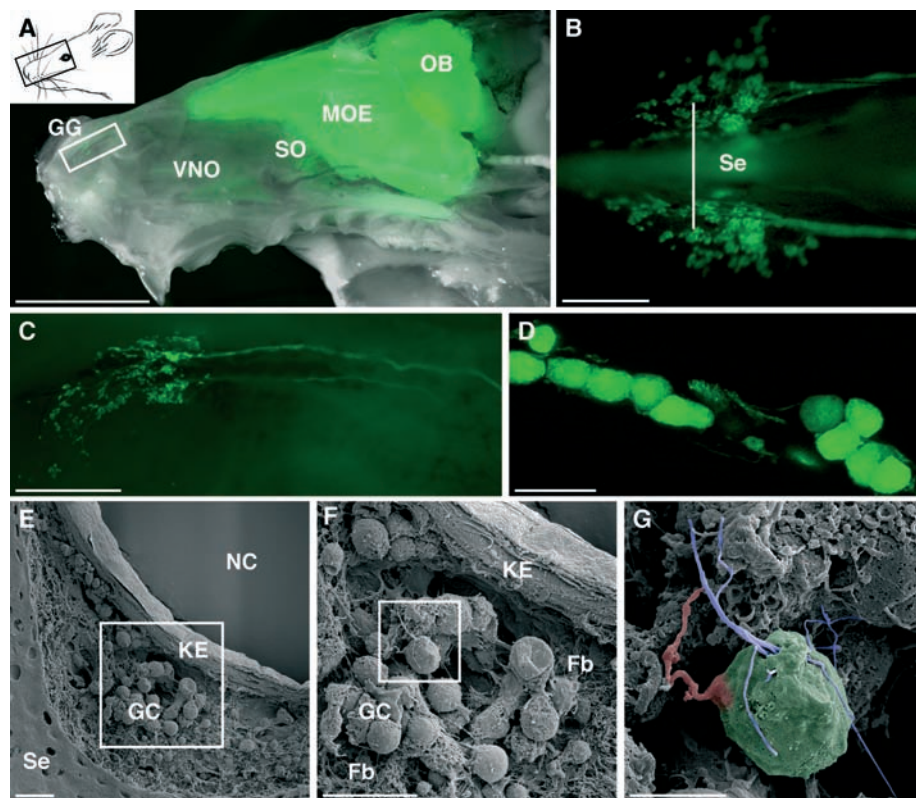

Fig. 1. Ciliary processes are present on the mouse GG cells. (**A**) Sagittal section through the nasal cavity of an OMP-GFP mouse: Neurons from the main olfactory epithelium (MOE), septal organ (SO), VNO, and GG (white rectangle) project to the olfactory bulb (OB). (**B**) Dorsal view of the GG, an arrow-shaped parallel organ on both sides of the nasal septum (Se). (**C**) High-power view from one GG [rectangle in (A)]. (**D**) Maximum-intensity projection (12 μm) of a GG cell cluster by confocal microscopy. (**E**) SEM micrograph of a GG coronal section [line in (B)]. Clusters of GG cells (GC) are shown, located along the Se underneath the KE lining the nasal cavity (NC) [square detailed in (F)]. (**F**) Close-up view of the GG cells in a fibroblast meshwork (Fb) [square detailed in (G)]. (**G**) GG cell (false color green) with its axon (false color red) and thin ciliary processes (false color blue). Scale bars, 1 mm in (A); 0.1 mm in (B); 0.25 mm in (C); 25 μm in (D); 20 μm in (E) and (F); and 5 μm in (G).

Department of Pharmacology and Toxicology, University of Lausanne, Bugnon 27, CH-1005 Lausanne, Switzerland.

*To whom correspondence should be addressed. E-mail: mbroille@unil.ch

reach the nasal cavity. Immunostaining experiments confirmed the presence of multiple cilia on GG cells (fig. S1, H to K).

We tried to resolve the difference between the number of cilia observed with SEM versus TEM (4 to 8 versus 30 to 40) and found another cell population that trapped most cilia inside the ganglion structure (fig. S1, D and K). These cells have

a triangular shape with thin cytoplasmic extensions (Fig. 2A). Immunostaining experiments demonstrated the glial origin of the wrapping cells by positive staining for S100β (Fig. 2, B to D) and glial fibrillary acidic protein (fig. S4, A to C). The GFP-positive cells expressed the olfactory marker $G_{\alpha i2}$ (Fig. 2, E to G) and the neuronal marker βIII-tubulin (fig. S4, D to F). Thus, a GG comprises two

different cell populations: glial cells and neurons (GFP-positive cells), which bear multiple primary cilia, putative sites of chemosensory transduction.

By systematic scanning of the nasal cavity (fig. S5), we found that the KE covering the GG was already present at birth (mice aged 30 min); no cilia were found protruding into the airspace of the nasal cavity. The aspect of KE did not
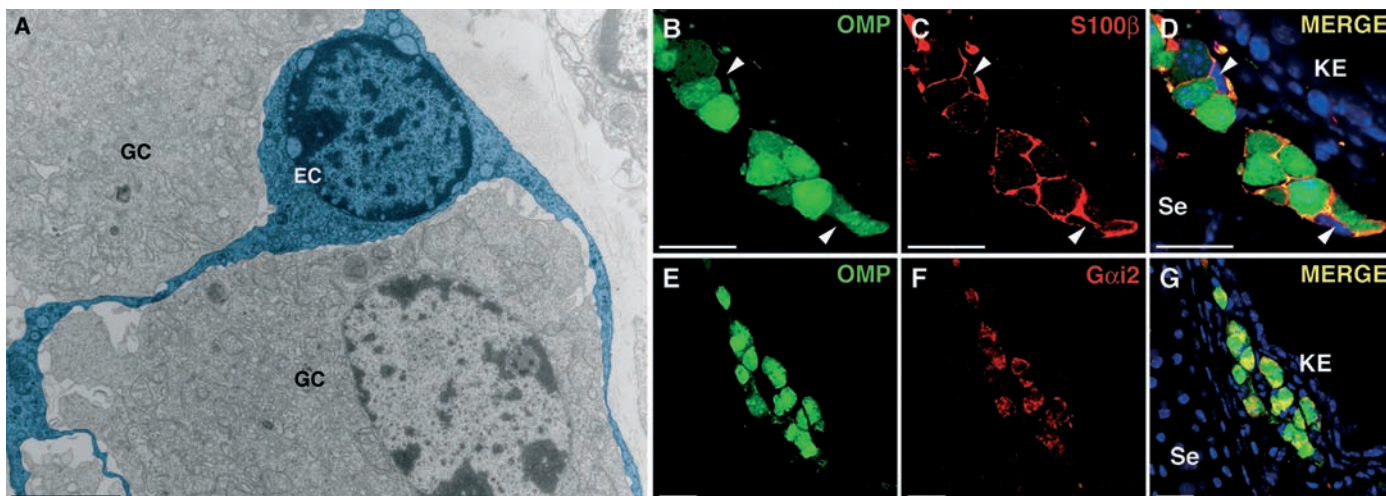

Fig. 2. The GG is composed of cells of different origins. (**A**) TEM micrograph confirming the presence of ensheathing cells (EC, false color blue) individually packaging GG cells (GC). An EC had a triangular cell body, a round nucleus, and long arms circling GG cells. (**B** to **G**) High-power views of glial or neuronal protein immunoreactivity. GG cells were recognized by their OMP-GFP expression [(B) and (E)]. (C) Glial marker S100β expressed in cells surrounding the GG cells. (D) Merge of (B) and (C). White arrowheads indicate GFP-negative glial cells [(B) to (D)]. (F) $G_{\alpha i2}$ staining in GG cells. (G) Merge of (E) and (F), where colocalization appears in yellow. Scale bars, 2 μm in (A) and 20 μm in (B) to (G).
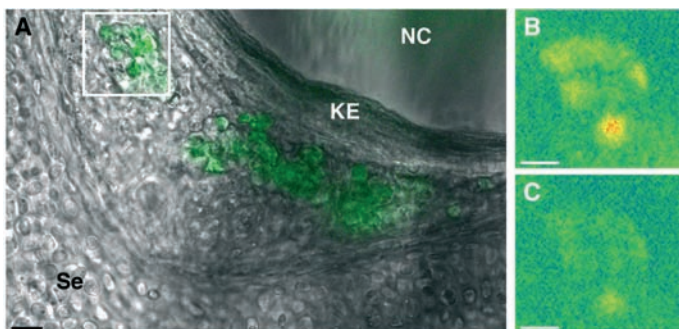

Fig. 3. APs activate GG cells. (**A**) Coronal slice from the GG region. (**B**) Uptake of Fura-2AM into GG cells within the white rectangle from (A), measured at 380 nm before (B) and at the peak of the intracellular calcium increase induced by a control pulse of KCl (**C**). (**D** to **E**) Lack of calcium transients after the perfusion of mouse milk (Milk), nipple wash (NW), a mix of odors and known mouse pheromones (Mix), or mouse urine. (**F**) APs but not general pheromones (GP) induced a reversible calcium transient. (**G**) AP response was abolished only after depletion of intracellular calcium stores by thapsigargin (Th, 20 mM) in divalent-free medium. Fluorescence intensity ratio (ΔF) = $F340/F380$. Perfusion times are indicated by horizontal bars in (D) to (G). Scale bars, 20 μm in (A) and 10 μm in (B) and (C).
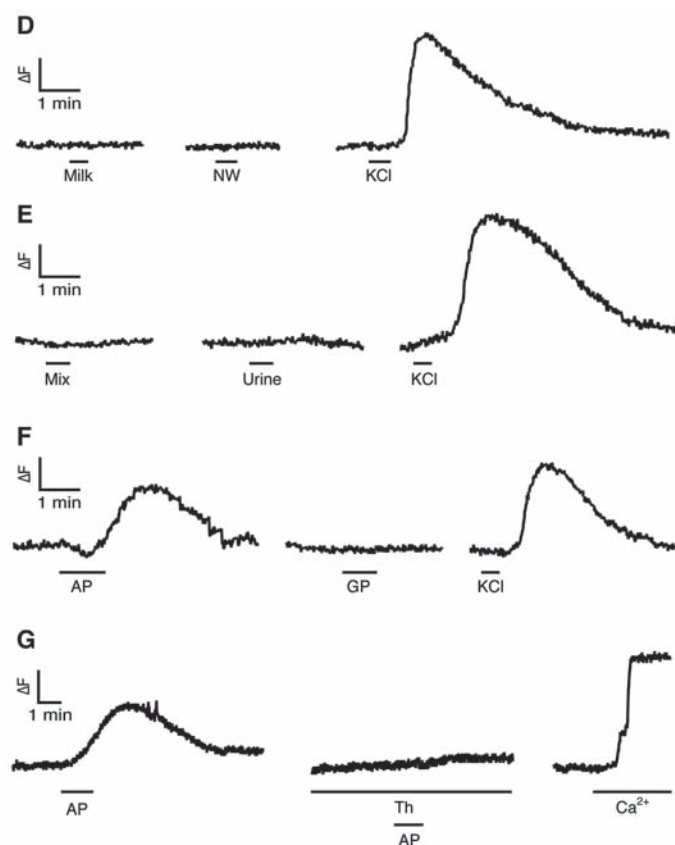
change with aging (fig. S5, B to D). To assess how potential chemosensory stimuli could reach and activate GG cells, we performed standard skin permeability assays using Toluidine blue (fig. S6, A to C) and Lucifer yellow (fig. S6, D and E). In contrast to the control (the back skin of the same animal) (fig. S6D), the KE covering the GG cells was found to be permeable by hydrophilic substances, suggesting that water-soluble chemostimuli have access to the outside zone of the GG cell clusters, where primary cilia are located (fig. S6E). A similar morphological situation is observed in *Caenorhabditis elegans*, in which the cilia of the amphid chemosensory neurons (AWA, AWB, and AWC), located under the cuticle, sense volatile and hydrophilic odors via direct diffusion (*20*).

Focusing on its potential water-soluble quality, we used calcium imaging on coronal slices to identify the GG chemostimulus (Fig. 3). Tissue slices were incubated in Fura-2 acetoxymethyl ester (AM), a calcium-sensitive dye. GG cells were identified by the intrinsic green fluorescence of GFP in their cell bodies (Fig. 3A), and the uptake of the dye was confirmed by fluorescence measurements (Fig. 3B). Chemical stimuli were delivered in oxycarbonated artificial cerebrospinal fluid (ACSF) continuously perfused on the tissue slices in the imaging chamber. Cell viability was assessed by pulses of KCl (Fig. 3, C to F). Various hypotheses have been made concerning the possible GG function, the most favorite being its role in mother-pup recognition (*10*, *11*, *14*) because of its presence at birth (*11*) and axonal wiring to the necklace glomeruli of the olfactory bulb implicated in newborn suckling behavior (*21*). However, we did not record any calcium increase with mouse milk (*n* = 24 cells, 4 mice) or mammary secretions (*n* = 29 cells, 5 mice) from lactating female mice (Fig. 3D). A mix of odors and known isolated mouse pheromones (*22*) (*n* = 43 cells, 15 mice) or mouse urine as the major source of pheromones (*n* = 29 cells, 9 mice) did not enhance fluorescence (Fig. 3E). Looking for other volatile and water-soluble stimuli to test on GG cells, we noticed that the intraspecies danger signals, the so-called APs, released by stressed animals are known to have these physical characteristics (*8*, *9*). We collected APs during killing of mice with CO_2, which is known to be a major stress factor (*23*). The perfusion of APs induced a reversible fluorescence enhancement in almost all tested GG cells from newborn and adult mice (*n* = 39 out of 41 cells, 7 mice; Fig. 3F). As a control, general pheromones (GPs) collected from mice

freely behaving and communicating, when no stress was applied, did not induce any calcium increase (*n* = 25 cells, 5 mice; Fig. 3F) and neither did CO_2 itself (*24*) (*n* = 26 cells, 5 mice) or other hypothesized stimuli (*10–14*) such as acidification (pH = 6) (*n* = 19 cells, 3 mice) or temperature changes (from 37° to 4°C) (*n* = 5 cells, 2 mice) (fig. S7).

We investigated the origin of the calcium increase observed in the presence of APs and found that it could be recorded in divalent-free ACSF solution (*n* = 26 cells, 6 mice; Fig. 3G), indicating that it was generated preferentially by Ca^{2+} released from intracellular stores and not only by external calcium influx. Depletion of Ca^{2+} stores by thapsigargin (20 mM), an inhibitor of the microsomal Ca^{2+}-ATPases (*25*), abolished the response to APs (*n* = 8 cells, 2 mice; Fig. 3G). At the end of these experiments, perfusion of ACSF containing calcium (2 mM) induced an overshoot of the intracellular calcium concentration, confirming the previous opening of store-operated calcium channels. Thus, contrary to olfactory neurons, GG cells, with their primary cilia localized in an extracellular matrix made of type IV collagen and not in a mucus layer (fig. S1), can act independently from the calcium concentration present in their environment.

We next addressed the question of the behavioral relevance of AP sensing by GG cells. The isolated nature of the GG makes it suitable for lesion experiments, allowing axonal projection bundles of GG cells to be sectioned (axotomy) (*11*). After surgery, pups were given back to their mothers and mother-pup recognition was not affected by the procedure. Thirty days after the lesion, we tested whether APs able to activate a calcium increase in GG cells (ACSF + AP) also modified mice behavior in vivo (Fig. 4). APs induce a typical freezing reaction in rodents (*26*). Such a reaction was observed in control mice (*n* = 6) placed in a closed Plexiglas container in the presence of ACSF + AP (Fig. 4, A and B, and movie S1). After axonal lesions (Axo mice, *n* = 5; Fig. 4C), this behavior was replaced by exploring activity. These Axo mice were not affected anymore by the presence of APs in their environment (Fig. 4D and movie S2). Control and lesioned mice were equally efficient at finding a buried cookie in the bedding (Fig. 4E).

Pheromonal communication plays an important role in social interactions among individuals of the same species, affecting, in particular, sexual, territorial, and maternal behaviors (*27*). We morphologically characterized the GG and identified it as the olfactory subsystem mediating AP detection in neonate and adult mice. To perform this primordial function, the GG has a specialized and basic morphology: a ganglion protected from the external world by water-permeable keratin. The GG acts as a warning system dedicated to the recognition of short-lived molecules encoding danger. These molecules require immediate attention. The unusual location of the GG at the tip of the nose, far from the main olfactory system,
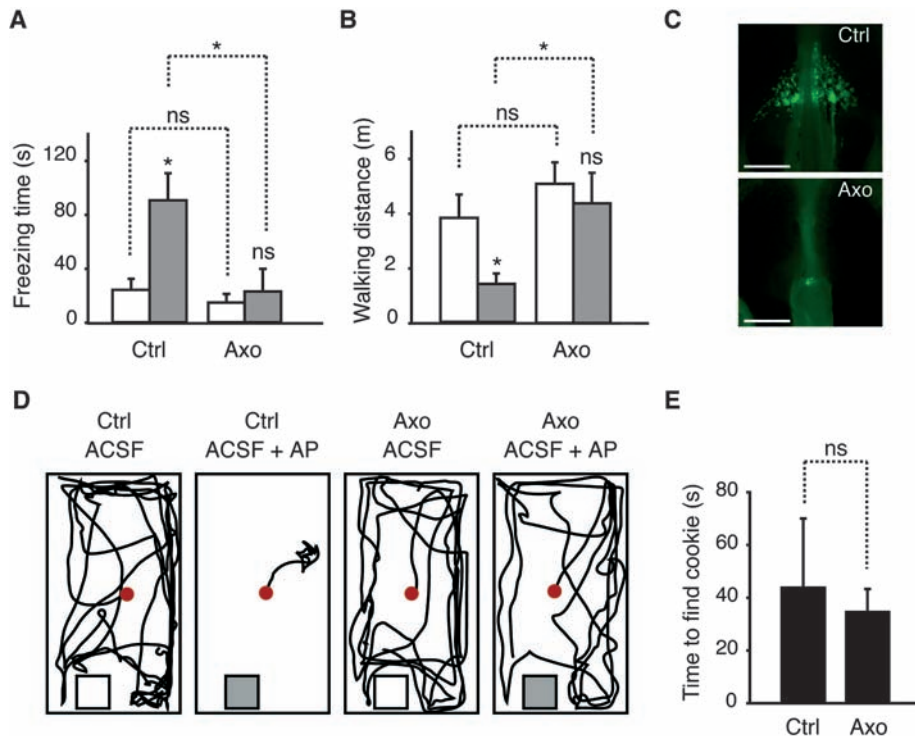

Fig. 4. AP sensing depends on a functional GG. (**A** and **B**) APs in ACSF solution (white bars, ACSF; gray bars, ACSF + AP) induced a significant increase in freezing behavior and a decrease in walking distance in control (Ctrl) but not in axotomized (Axo) OMP-GFP mice. (**C**) Whole-mount dorsal views of the GG region from Ctrl and Axo mice. (**D**) Representative tracking of the walking distance covered by mice in the test chamber in the absence (white square) or presence (gray square) of APs in the ACSF container (square). Red dots indicate the position of the mice at the beginning of the 3-min test. (**E**) Olfactory function in finding the cookie was similar in both experimental groups. In (A), (B), and (E), error bars indicate the SEM of *n* = 5 to 6 observations, *P < 0.05; ns, not significant. Scale bars, 500 μm in (C).

allows the stimuli to be rapidly detected. AP sensing is a conserved modality that is present from primitive organisms such as worms (*28*) to humans (*29*). The presence of a GG has been identified in all mammalian species looked at so far, including humans (*15, 30*). When produced by a conspecific, APs play an important role in increasing overall species fitness (*31*).

References and Notes

1. M. H. Beale *et al.*, *Proc. Natl. Acad. Sci. U.S.A.* **103**, 10509 (2006).
2. M. K. Stowe, T. C. Turlings, J. H. Loughrin, W. J. Lewis, J. H. Tumlinson, *Proc. Natl. Acad. Sci. U.S.A.* **92**, 23 (1995).
3. M. Ono, H. Terabe, H. Hori, M. Sasaki, *Nature* **424**, 637 (2003).
4. R. S. Mirza, D. P. Chivers, *J. Chem. Ecol.* **27**, 1641 (2001).
5. A. G. Gutierrez-Garcia, C. M. Contreras, M. R. Mendoza-Lopez, O. Garcia-Barradas, J. S. Cruz-Sanchez, *Physiol. Behav.* **91**, 166 (2007).
6. A. Boissy, C. Terlouw, P. Le Neindre, *Physiol. Behav.* **63**, 489 (1998).
7. C. Zalaquett, D. Thiessen, *Physiol. Behav.* **50**, 221 (1991).
8. Y. Kiyokawa, T. Kikusui, Y. Takeuchi, Y. Mori, *Chem. Senses* **30**, 513 (2005).
9. E. L. Abel, *Physiol. Behav.* **50**, 723 (1991).
10. D. S. Koos, S. E. Fraser, *Neuroreport* **16**, 1929 (2005).
11. D. Roppolo, V. Ribaud, V. P. Jungo, C. Luscher, I. Rodriguez, *Eur. J. Neurosci.* **23**, 2887 (2006).
12. S. H. Fuss, M. Omura, P. Mombaerts, *Eur. J. Neurosci.* **22**, 2649 (2005).
13. M. J. Storan, B. Key, *J. Comp. Neurol.* **494**, 834 (2006).
14. J. Fleischer, N. Hass, K. Schwarzenbacher, S. Besser, H. Breer, *Histochem. Cell Biol.* **125**, 337 (2006).
15. H. Grueneberg, *Z. Anat. Entwicklungsgesch.* **140**, 39 (1973).
16. J. Fleischer, K. Schwarzenbacher, H. Breer, *Chem. Senses* **32**, 623 (2007).
17. J. Fleischer, K. Schwarzenbacher, S. Besser, N. Hass, H. Breer, *J. Neurochem.* **98**, 543 (2006).
18. H. A. Praetorius, K. R. Spring, *Annu. Rev. Physiol.* **67**, 515 (2005).
19. V. Singla, J. F. Reiter, *Science* **313**, 629 (2006).
20. C. I. Bargmann, H. R. Horvitz, *Cell* **74**, 515 (1993).
21. K. Shinoda, Y. Shiotani, Y. Osawa, *J. Comp. Neurol.* **284**, 362 (1989).
22. T. Leinders-Zufall *et al.*, *Nature* **405**, 792 (2000).
23. M. C. Leach, V. A. Bowell, T. F. Allan, D. B. Morton, *Comp. Med.* **52**, 249 (2002).
24. J. Hu *et al.*, *Science* **317**, 953 (2007).
25. C. Mathes, S. H. Thompson, *J. Gen. Physiol.* **106**, 975 (1995).
26. T. Kikusui, S. Takigami, Y. Takeuchi, Y. Mori, *Physiol. Behav.* **72**, 45 (2001).
27. P. A. Brennan, F. Zufall, *Nature* **444**, 308 (2006).
28. B. D. Wisenden, M. C. Millard, *Anim. Behav.* **62**, 761 (2001).
29. R. Hauser *et al.*, *Forensic Sci. Int.* **155**, 226 (2005).
30. T. Tachibana, N. Fujiwara, T. Nawa, *Arch. Histol. Cytol.* **53**, 147 (1990).
31. E. B. Mondor, B. D. Roitberg, *Proc. R. Soc. London Ser. B* **271**, S341 (2004).
32. We thank I. Rodriguez for the OMP-GFP mice; J. and S. Fakan for their enthusiastic help with EM techniques and for analyzing EM micrographs; G. Knott, A. Mucciolo, and S. Rosset for preparing EM tissue samples; the Cellular Imaging Facility of the University of Lausanne and its coordinator J.-Y. Chatton for valuable advice; C. Lebrand for providing antibodies; N. Rosenblatt-Velin for help with animal handling; and K. Geering and R. Stoop for fruitful discussions on the manuscript. Supported by the Department of Pharmacology and Toxicology, the Swiss National Science Foundation, and the Leenaards Foundation.

Control of the Reversibility of Cellular Quiescence by the Transcriptional Repressor HES1

Liyun Sang,[1,2] Hilary A. Coller,[3] James M. Roberts[1,4]*

The mechanisms by which quiescent cells, including adult stem cells, preserve their ability to resume proliferation after weeks or even years of cell cycle arrest are not known. We report that reversibility is not a passive property of nondividing cells, because enforced cell cycle arrest for a period as brief as 4 days initiates spontaneous, premature, and irreversible senescence. Increased expression of the gene encoding the basic helix-loop-helix protein HES1 was required for quiescence to be reversible, because HES1 prevented both premature senescence and inappropriate differentiation in quiescent fibroblasts. In some human tumors, the HES1 pathway was activated, which allowed these cells to evade differentiation and irreversible cell cycle arrest. We conclude that HES1 safeguards against irreversible cell cycle exit both during normal cellular quiescence and pathologically in the setting of tumorigenesis.

Reversibility is a defining characteristic of cellular quiescence: In contrast to cells in other nonproliferating states, including terminal differentiation and senescence, only quiescent cells normally retain the ability to resume proliferation. Cells entering each of these arrested states stop the cell division cycle by increasing the abundance of cell cycle inhibitory proteins, such as cyclin-dependent kinase (CDK) inhibitors (*1–5*), yet it is only in quiescent cells that this block to proliferation can be reversed. Expression of CDK inhibitors is sufficient to enforce a nondividing state (*1*), and depletion of these proteins can disrupt quiescence in many cells, including hematopoietic stem cells (*6, 7*). However, ectopic expression of CDK inhibitors does not recapitulate the transcriptional signature of quiescent cells (*8*), which suggested that cell cycle arrest and cellular quiescence are not functionally equivalent.

The amount of the CDK inhibitor p21^{Cip1} (p21) is increased in fibroblasts that become quiescent in response to serum starvation or cell-cell contact (fig. S1A). To determine whether regulated expression of p21 would induce a reversible, quiescent-like cell cycle arrest,

we used retroviral-mediated gene transduction to introduce into proliferating early-passage human lung fibroblasts a p21 expression cassette flanked by loxP sites (loxp-p21) (fig. S2A). Expression of p21 from this cassette efficiently blocked S-phase entry (Fig. 1A). Four days later, we reversed the increase in p21 abundance by infecting the cells with a vector expressing a cre recombinase–green fluorescent fusion protein (cre-GFP). Six days later, more than 95% of the cells showed fluorescence from GFP, and the expression of p21 had returned to the baseline level found in proliferating cells (Fig. 1B). Nevertheless, these cells failed to reenter the cell cycle (Fig. 1A), expressed increased amounts of the senescence-associated enzyme β-galactosidase (Fig. 1C), and formed senescence-associated heterochromatin foci (SAHF) (Fig. 1J). As a control, we also transduced cells with an empty loxp vector and arrested them by contact inhibition for 4 days. After infection with cre-GFP, more than 95% of the cells showed fluorescence from GFP. These cells resumed proliferation efficiently after release from contact inhibition (Fig. 1D) and did not display a senescent-like morphology. These experiments showed that sustained (4 days or longer) expression of p21 induced an irreversible senescent-like state. We thus explored the mechanism by which quiescent cells avoid this fate despite their constitutive expression of p21.

We previously used gene expression profiling to observe that the transcriptional repressor Hairy and Enhancer of Split1 (HES1) is transcriptionally regulated in quiescent fibroblasts, but not in fibroblasts that have undergone cell cycle arrest in response to ectopic expression of CDK inhibitory proteins (*8*). We confirmed

[1]Division of Basic Sciences, Fred Hutchinson Cancer Research Center, Seattle, WA 98109, USA. [2]Molecular and Cellular Biology Program, University of Washington, Seattle, WA 98195, USA. [3]Department of Molecular Biology, Princeton University, Princeton, NJ 08544, USA. [4]Department of Biochemistry, University of Washington, Seattle, WA 98195, USA.

*To whom correspondence should be addressed. E-mail: jroberts@fhcrc.org

ERRATUM

Post date 20 November 2009

Reports: "Grueneberg ganglion cells mediate alarm pheromone detection in mice" by J. Brechbühl *et al.* (22 August 2008, p. 1092). The next-to-last sentence of the text read "The presence of a GG has been identified in all mammalian species looked at so far, including humans (*15, 30*)." Instead, it should read "The presence of a GG has been identified in all mammalian orders looked at so far, including human embryos (*15, 30*)."